Chem Catalysis

CellPress

Perspective

Synergistic effects in organic mixtures for enhanced catalytic hydrogenation and hydrodeoxygenation

Ankit Mathanker,[1,2,3] Sahil Halarnkar,[1,2,3] Bolton Tran,[1,2] Nirala Singh,[1,2,*] and Bryan R. Goldsmith[1,2,*]
[1]Department of Chemical Engineering, University of Michigan, Ann Arbor, MI 48109-2136, USA
[2]Catalysis Science and Technology Institute, University of Michigan, Ann Arbor, MI 48109-2136, USA
[3]These authors contributed equally
*Correspondence: snirala@umich.edu (N.S.), bgoldsm@umich.edu (B.R.G.)
https://doi.org/10.1016/j.checat.2024.101135

THE BIGGER PICTURE Challenges and opportunities:

- There is a practical need for the hydrogenation and hydrodeoxygenation of organic mixtures to value-added products such as fuels and chemicals
- Organic mixtures may have simple or complex mutual influences that cause the catalytic rate and selectivity to be different compared to converting a single organic species
- Future work should study the catalytic conversion of binary organic mixtures to elucidate the simple and complex mutual interactions

SUMMARY

The hydrogenation and hydrodeoxygenation (HDO) of organic mixtures are important processes in bio-oil conversion and plastics upcycling. Understanding how the presence of co-reactants in organic mixtures affects the kinetics is critical for designing reactors that can convert these mixtures into desired products. Here, we discuss cases in (electro)catalysis where the presence of a co-reactant R_2 enhances the rate of hydrogenation or HDO of another reactant R_1 beyond the rate if only R_1 is present. We divide the discussion into simple and complex mutual influences. Simple mutual influences occur when the presence of R_2 does not change the mechanism or values of rate constants of elementary steps for R_1. A complex mutual influence of R_2 on R_1 occurs if the presence of R_2 changes the rate constants of elementary steps involving R_1. We discuss challenges and opportunities in discerning the different mutual influences and increasing their synergistic effects in organic mixtures.

INTRODUCTION

Catalytic hydrogenation and hydrodeoxygenation (HDO) of organic mixtures are important for biomass and plastics conversion into sustainable chemicals and fuels.[1,2] However, most fundamental kinetics studies of catalytic hydrogenation and HDO involve examining the conversion of a single organic reactant, not organic mixtures.[3,4] Bridging the knowledge gap between catalytic studies of a single organic molecule and more applied studies of complex organic mixtures is needed for improving applications such as electrocatalytic and thermocatalytic bio-oil upgrading. One way to start bridging this knowledge gap is to understand how the kinetics of organic reactions in simpler organic mixtures are mutually influenced by the different organics involved.[5–7] This knowledge is crucial for designing catalytic reactors that can convert these streams of organic mixtures in a desired route.

In organic mixtures, an over-approximation may be that the rates of conversion for two reactants are independent of one another; that is, if R_1 is converted with a turnover frequency (TOF) of 1 s^{-1} individually, and R_2 is converted at 1.5 s^{-1} individually, then, if they were mixed and kept at the same original concentration and operating conditions, they would each retain the same TOF. This approximation is often incorrect for heterogeneous catalysis, particularly if R_1 and R_2 compete for the same surface catalyst sites. In these cases, it is widely found that the rate of conversion in the mixture would result in lower rates for both reactants, or perhaps one reactant is converted at a similar rate but the other rate is decreased.[7–9] We refer to a decrease in the rate in the mixture relative to the individual species as an antagonistic effect. Other types of synergistic effects within these organic mixtures during catalytic conversion are also possible, and understanding their prevalence and quantitative impact on catalytic activity and selectivity is of broad relevance.

In this perspective, we discuss cases of antagonistic effects in mixtures as well as the more non-intuitive examples where rates are accelerated in mixtures, which we refer to as enhancement or synergistic effects. We organize our discussion around simple (where R_2 reacts but does not interact with R_1) and complex (where R_2 may or may not react but does interact with R_1) mutual influences in (electro)catalytic reactions.[5] Simple mutual influences occur when the presence of a co-reactant does not change the reaction mechanism or values of rate constants of elementary steps. Simple mutual influences include competitive adsorption lowering the rate of reaction (antagonistic effect) or an acceleration of the reaction (enhancement/synergistic effect) based on peculiarities of competitive reaction kinetics. An example of a simple mutual influence causing an enhancement effect for hydrogenation or HDO of a reactant R_1 is when a second reactant R_2 reacts with adsorbed hydrogen to increase the number of free sites, allowing the coverage of R_1 to increase. We show mathematically that, for the same set of reactants (R_1 and R_2), a simple mutual influence can cause either an antagonistic or synergistic effect depending on the reaction conditions. A complex mutual influence of R_2 on R_1 occurs if the presence of R_2 causes a change in the adsorption strength of R_1, modifies the local environment or the electronic structure of the catalyst, or introduces a new elementary step involving R_1. All of these effects can lead to a change in the reaction mechanism or the rate constants of elementary steps, categorizing them as complex mutual influences. These complex mutual influences may arise because of strong interactions between co-reactants, such as hydrogen bonding, whereas simple mutual influences do not require interacting co-reactants but only consumption of surface species. We highlight challenges and opportunities in elucidating mutual influences and increasing the synergistic effects on catalytic activity in organic mixtures.

Simple mutual influences

Following the principle of Occam's razor, we will begin by considering kinetics that can be rationalized by models considering only simple mutual influences. It is important to understand the magnitude of synergistic or antagonistic effects on the reaction rates and product selectivity that are possible from simple mutual influences. Additionally, it would be useful if there were a set of guidelines to know if a reaction can be explained solely by simple mutual influence or requires complex mutual influences to be invoked. Here, we give our perspective on these matters, supported by several case studies.

Competitive adsorption of organics species causing decreased coverage and lower reaction rates is the most observed simple mutual influence in mixtures undergoing catalytic conversion. In this case, the adsorption of R_2 hinders the adsorption of R_1 by blocking catalyst sites during the reaction of a mixture of R_1 and R_2. This competitive adsorption creates an antagonistic effect that decreases the rate of reaction for R_1, R_2, or all reactants involved. For example, CO adsorption on Pt active sites during bio-oil hydrogenation inhibits the hydrogenation of phenol to cyclohexanol.[8] Similarly, the yield of phenol HDO is suppressed by methyl heptanoate during their simultaneous reactions over a sulfided NiMo/γ-Al_2O_3 catalyst.[9] Likewise, strong furfural adsorption on Ni/SiO_2 during furfural-guaiacol co-HDO suppresses the guaiacol HDO reaction rate.[7] A simple set of elementary steps describing these Langmuir-Hinshelwood (LH) reactions may be

$$H + * \rightleftarrows H* \quad \text{(Equation 1)}$$

$$R_1 + * \rightleftarrows R_1* \quad \text{(Equation 2)}$$

$$H* + R_1* \rightarrow 2* + R_1H \quad \text{(Equation 3)}$$

$$R_2 + * \rightleftarrows R_2* \quad \text{(Equation 4)}$$

$$H* + R_2* \rightarrow 2* + R_2H \quad \text{(Equation 5)}$$

where H represents a hydrogen equivalent that competes for free sites (*) with reactant R_1 and co-reactant R_2. For electrocatalytic hydrogenation, the H comes from the reduction of water or protons, whereas for catalytic hydrogenation, it comes from H_2.[10,11] A common approach is to assume that all adsorption steps are quasi-equilibrated (Equations 1, 2, and 4) so that the reaction rate r for R_1 would be (derived in Note S1)

$$r_{R_1} = \frac{k_3 K_2 K_1 C_{R_1} C_H}{\left(1 + K_1 C_H + K_2 C_{R_1} + K_4 C_{R_2}\right)^2} \quad \text{(Equation 6)}$$

Here, k_3 is the rate constant for the surface reaction to form R_1H, K_2 is the equilibrium constant for the adsorption of R_1, C_{R_1} is the concentration of R_1, K_1 is the equilibrium constant for the adsorption of the hydrogen equivalent H, C_H is the concentration of the hydrogen equivalent, K_4 is the equilibrium constant for the adsorption of R_2, and C_{R_2} is the concentration of R_2. By convention, we normalize r_{R_1} to the total number of active sites on the catalyst so that r_{R_1} is a TOF. Rate constants k_i and k_{-i} correspond to forward and reverse rate constants for elementary step i, respectively. Under the assumption that the surface reaction is rate determining, it is evident from Equation 6 that the presence of R_2 can only decrease the rate of reaction of R_1.

A less intuitive simple mutual influence is the acceleration of a reaction based on peculiarities of competitive reaction kinetics. Pyatnitsky showed that, for a given reaction mechanism, a set of rate parameters and reactant concentrations exists for which an enhancement effect of one reactant on the other, or an enhancement effect on both reactants, can be achieved.[5] This finding suggests that it is possible to observe an enhancement in the reaction rate for R_1 by increasing the concentration of R_2 within a defined bound. For example, NO reduction by CO was accelerated by O_2 on Pd and Pt/Al_2O_3 despite NO and O_2 competing for catalyst sites and reduction equivalents. In this case, NO, O_2, and CO represent R_1, R_2, and H, respectively, in the reaction mechanism above. This acceleration effect is only explained by a rate law if we do not assume that adsorption steps are quasi-equilibrated. By applying the pseudo-steady-state hypothesis, the derived rate for R_1 can be increased by the presence of R_2. We show the derivation in Note S2. In this derivation, the reaction mechanism and rate constants for elementary steps are assumed to be unaffected by the presence

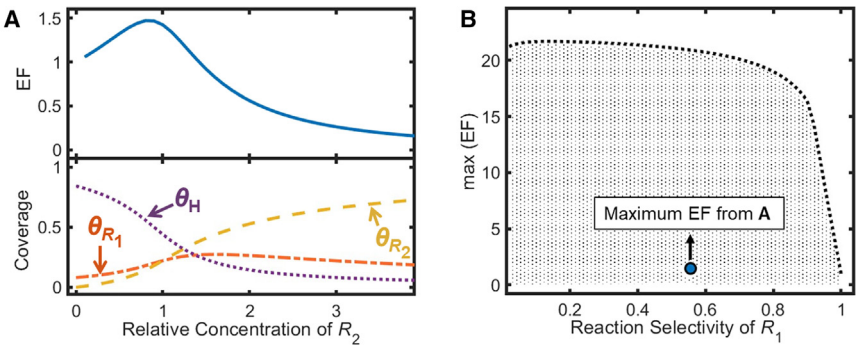

Figure 1. Enhancement factor through simple mutual influence for an LH reaction

(A) The enhancement factor (EF; blue) versus relative R_2 concentration ($=C_{R_2}/C_{R_1}$), alongside coverage for R_1 (dot-dashed orange line), R_2 (dashed yellow line), and H (dotted purple line). Values of rate constants and concentrations are as follows: $C_{R_1} = 1$, $C_H = 1$, $k_1 = 2$, $k_{-1} = 0.1$, $k_2 = 1$, $k_{-2} = 0.1$, $k_3 = 1$, $k_4 = 1$, $k_{-4} = 0.1$, and $k_5 = 1$. The model details are described in Note S2.

(B) Pareto frontier to maximize EF for different values of R_1 selectivity ($=r_{R_1}/[r_{R_1} + r_{R_2}]$). The dotted line represents the maximum EF that can be obtained from simple mutual influences under the bounds used here. The bounds used for the rate parameters and concentrations are [0.01, 10] and [0.01, 1], respectively. The highest EF value from (A) is denoted by a blue circle.

of R_2, which is why we refer to this acceleration as a synergistic "simple" mutual influence. Because this simple mutual influence depends wholly on the rate parameters, concentrations, and the underlying reaction mechanism, we expect similar effects in other reactions following the same LH mechanism. Hydrogenation and HDO of organics have been observed to follow the LH reaction mechanism, making them eligible for this type of simple mutual influence. Through mathematical modeling, we demonstrate that the LH mechanism can exhibit a rate enhancement for all reactants involved.

We show here that these rate enhancements occur because, under certain conditions, counterintuitively, the presence of R_2 increases the coverage of R_1 (θ_{R_1}). We highlight that a simple mutual influence can lead to a rate enhancement of R_1 even without the need to invoke any common effects, such as changes in the adsorption strength of R_1 or solvent environment near R_1 in the presence of R_2. The data in Figure 1A show the rate enhancement and coverage based on an LH reaction mechanism (Equations 1, 2, 3, 4, and 5). The enhancement factor (EF) is defined as the ratio of the reaction rate of R_1 in the presence of R_2 to the reaction rate of R_1 with no R_2 in the mixture (Equation 7). Figure 1A is divided into two regimes depending on whether the EF is greater than or less than 1. An EF greater than 1 indicates a synergistic effect on R_1 by R_2, whereas an EF of less than 1 corresponds to an antagonistic effect as the reaction suffers from competitive adsorption. These simple mutual effects can be explained by observing the trends in coverage for R_1 (θ_{R_1}), R_2 (θ_{R_2}), and H (θ_H) as a function of R_2 concentration. In both regimes, an increasing R_2 concentration leads to a higher R_2 coverage. Consequently, the coverage of H drops because of the reaction with R_2 (Equation 5). In the synergistic regime at lower concentrations of R_2 in Figure 1A, this drop in H coverage is met by an increase in R_1 coverage, which leads to a larger reaction rate for R_1. The increase in θ_{R_1} in this regime with increasing R_2 concentration may seem counterintuitive, but it is a result of R_2 reacting with H and freeing catalyst sites that R_1 can then occupy.

$$\mathrm{EF} = \frac{r_{R_1(C_{R_2})}}{r_{R_1(C_{R_2}=0)}} \qquad \text{(Equation 7)}$$

At larger R_2 concentrations in the antagonistic regime, a decrease in R_1 coverage is observed, which leads to smaller R_1 reaction rates. This antagonistic regime behavior is similar to that expected by Equation 6, where R_2 blocks sites for R_1 and decreases r_{R_1}. By analyzing Figure 1A, we observe that, in the range of concentration of R_2 relative to R_1 of 0.9 to 1.4, the coverage of R_1 increases with increasing R_2 concentration, but the EF decreases. This behavior occurs because the rate of reaction for R_1 also depends on H coverage, which is decreasing. In Figure 1A, we can see that the EF has a large dependence on the relative concentration of R_2 based on the surface coverages of the various species involved. The synergistic regime (EF > 1) is observed when the coverage of H is larger than that of R_1.

A key takeaway is that a synergistic effect can only be observed if R_2 reacts with H; therefore, this mode of rate enhancement is limited by reaction selectivity. We define reaction selectivity as the ratio of the reaction rate of reactant R_1 to the sum of the reaction rates of R_1 and R_2. The enhancement in reaction rate for R_1 is always smaller than the increase in reaction rate for R_2. Another way to probe this tradeoff is by constructing a Pareto frontier (Note S5). The Pareto frontier in Figure 1B demonstrates the maximum theoretical EF possible for different reaction selectivities.[12,13] The maximum EF value is obtained by looking at possible rate parameters under the constraint that the rate constants of R_1 are not influenced by the presence of R_2 and determining the given set of rate parameters that give the highest EF. The maximum theoretical EF that can be obtained decreases as selectivity for R_1 increases. We note that Figure 1B depends on the bounds applied to the rate parameters and concentrations during optimization and, thus, should only be used to show general trends. The EF approaches 1 for high selectivity toward R_1. Approaching the maximum theoretical EF experimentally would require tuning each rate constant in the reaction mechanism, which is not possible currently. Other reaction mechanisms can only show synergistic enhancements by simple mutual enhancement if R_2 or adsorbed R_2 reacts with adsorbed H (Figure S1; Note S3). For example, for a mechanism such as proton-coupled electron transfer (PCET), where a proton directly reacts with R_2 without adsorption of H (Figure S2; Note S4), an EF is not observed because the reaction does not result in the clearing of catalyst sites. If R_1 is a PCET but R_2 is an LH mechanism, an EF is possible because R_2 reacting with adsorbed H will still open up available sites for R_1. A mutual acceleration for R_1 and R_2 can exist if both follow the LH model. A useful outcome of this Pareto frontier analysis is that, if an EF > 1

is observed but no R_2 is reacting (~100% reaction selectivity of R_1), then a simple mutual influence cannot explain the behavior, and a complex mutual influence must be occurring.

Complex mutual influences

Here we discuss case studies of (electro)catalytic reactions that highlight complex mutual influences. Complex mutual influences can occur in organic mixtures due to two types of interactions: direct interactions, such as hydrogen bonding or van der Waals between co-reactants, and indirect interactions, which occur through changing the local environment around R_1. These complex mutual influences may lower the energy of transition states,[14,15] enhance the adsorption strength of the reactant and intermediates,[7,16,17] or change the preferred reaction pathway. Therefore, properly selecting co-reactants in organic mixtures with complex mutual influences could be a strategy to improve the overall rates or selectivity of the catalytic process. We wish to clarify here that, although we consider organic mixtures, we assume the presence of only a single phase of matter, meaning that the concentrations of the organics do not cause formation of a new phase.

Hydrogen bonding has been discussed as a possible synergistic complex mutual influence between a reactant and a co-reactant in organic mixtures. The hydrogenation TOFs of benzaldehyde on certain metal electrocatalysts increase in the presence of polar co-reactants such as substituted phenols and benzoic acid.[14] For example, the TOF for electrocatalytic hydrogenation of benzaldehyde on Pd/C increases with a decrease in the pK_a of the co-reactant, as shown in Figure 2A, with a max EF of 3 with benzoic acid as the co-reactant. There was no measurable conversion of the co-reactant (phenol, 2-fluorophenol, or benzoic acid) in this experimental study, which provides evidence that complex mutual influences were at play, not simple mutual influences. The hydrogen bond strength of the donor co-reactant increases linearly as the pK_a decreases.[18,19] Therefore, the increase in TOF with a decrease in the co-reactant pK_a is attributed to an increase in hydrogen bond strength between benzaldehyde and the co-reactant and an increase in local H_3O^+ concentration. The H-bonding with the co-reactant causes an increase in polarization of the carbonyl group in benzaldehyde, as shown in Figure 2B, where phenol changes the charge of the carbonyl group from -0.2 e^- to -0.3 e^- through H-bonding. This increase in the polarization of the carbonyl group, combined with the increase in local H_3O^+ concentration, facilitates the transfer of H^+ to the carbonyl group during hydrogenation. A similar study for furfural hydrogenation reported an increase in the TOF in the presence of phenol on Cu/C, Pd/C, and Rh/C (and no measurable phenol was converted).[20]

Organic reactants may adsorb to surfaces more strongly in mixtures because of organic/co-reactant interactions, such as van der Waals interactions, leading to increased surface coverage and higher reaction rates. The presence of guaiacol increases the rate of furfural HDO on Ni/SiO_2, attributed to stronger adsorption of furfural due to furfural-guaiacol van der Waals interactions. The absence of guaiacol conversion with furfural present suggests that a complex mutual influence is occurring. The rate of HDO of furfural increased by an EF of 2.7 in the presence of 0.575 M guaiacol, as shown in Figure 2C. By fitting the rate data to a rate equation obtained for an LH mechanism, it was calculated that the adsorption equilibrium constant for furfural and its reaction intermediate increased 2.6 times with guaiacol addition (0.23 M furfural/0.23 M guaiacol ratio). Density functional theory (DFT) calculations predict that both furfural and guaiacol have similar adsorption strength on Ni(111), but the presence of guaiacol (Figure 2D) increases the adsorption strength of furfural by 11 kJ mol^{-1}, thus increasing furfural coverage and the overall reaction rate. We note that these absolute values of adsorption energies are overestimated due to the lack of including the enthalpic penalty for solvent displacement during adsorption of organics,[22] but the qualitative trends should stay the same.

A third cause of complex mutual influence is if a new reaction pathway arises in mixtures with two organics. Two different routes for the hydrogenation of benzaldehyde to benzyl alcohol were predicted by *ab initio* molecular dynamics, depending on whether phenol is present.[14,21] Benzaldehyde in the absence of phenol reacts with adsorbed hydrogen to form adsorbed benzyl alcohol, as shown in Figure 2E. The rate-determining step for benzaldehyde to benzyl alcohol in the absence of phenol is H addition to O via an LH step.[21] In contrast, benzaldehyde in the presence of phenol is hydrogenated to form adsorbed benzyl alcohol through a PCET step, as shown in Figure 2F. This different mechanism could rationalize the increased activity for benzaldehyde conversion in the presence of phenol.[14]

Opportunities for progress

Numerous electro(catalytic) processes would benefit from the ability to convert organic mixtures rather than pure streams.[23–25] Understanding mutual influences between two organics is a necessary step to fundamentally understand mutual influences in more complex mixtures such as bio-oil, which can contain more than 20 organics as reactants. Mutual influences are likely a common phenomenon in such systems, yet the individual contributions of simple and complex mutual influences on a reaction are difficult to quantify. Focused studies using experimental and computational approaches would help us to better understand and use the mutual influences of organics in (electro)catalytic reactions such as hydrogenation and HDO.

Controlled intrinsic kinetic experiments in the absence of mass or heat transport artifacts should be conducted on single organic reactants as well as mixtures to identify if there is any EF at all (Figure 3A). A high external mass transport for fast transport of species to and from the surface can be achieved by the analysis of dimensionless groups such as the Sherwood number, which accounts for the design parameters of the reactor, fluid velocity, and diffusion. The change in reaction rate due to internal mass transport for catalytic sites with micropores should be accounted for by correcting for pore diffusion using the internal effectiveness factor.[3] Heat transport artifacts can be minimized by operating at differential conditions to ensure a negligible change in bulk temperature due to the heat of the reaction. Before attributing the EF of an organic mixture to simple or complex influences, it is useful to have detailed knowledge about the reaction mechanism, associated rate parameters, and steady-state rate information of the individual reactions of R_1 and R_2. After individual rate constants for R_1 and R_2 are obtained,

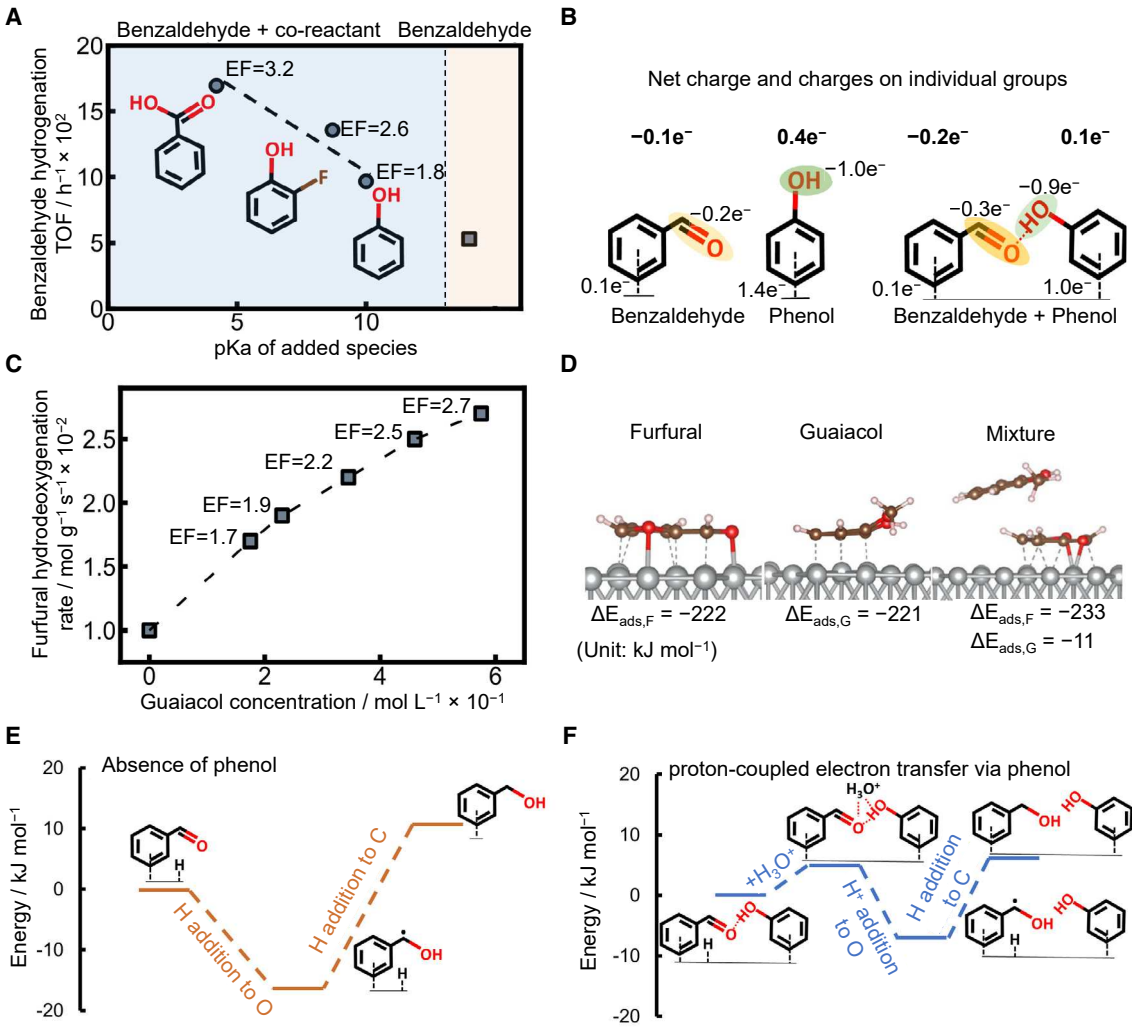

Figure 2. Complex mutual influences between a reactant and co-reactant

(A) Turnover frequency (TOF) for benzaldehyde hydrogenation in the presence of different co-reactant organics on Pd/C. The TOF for benzaldehyde hydrogenation in the absence of co-reactant is shown at the right. Reaction condition: sodium acetate-acetic acid (3 M, pH 5.2), 20 mM benzaldehyde, 20 mM co-reactant, 298 K, 1 bar N_2, and −0.1 V vs. reversible hydrogen electrode (RHE). The EF is mentioned for each data point.

(B) Net charges on the organics and individual group charges on the carbonyl group of benzaldehyde, hydroxyl group of phenol, and phenyl rings when adsorbed individually and adjacent on Pd(111).[14] Copyright 2020, John Wiley & Sons.

(C) Thermocatalytic hydrodeoxygenation rate of furfural at 30% conversion on Ni/SiO_2 versus the concentration of guaiacol. Furfural concentration = 0.23 mol L^{-1}. Temperature 250°C and 5 MPa H_2 pressure in a 300 mL stirred-batch reactor with an internal standard of 80 mL dioxane and 700 μL hexadecane.

(D) Most stable geometries of furfural (F), guaiacol (G), and adsorbed F in the presence of G on Ni(111) (ΔE_{ads}, density functional theory [DFT]-computed electronic adsorption strength in a vacuum).[7] Copyright 2021, American Chemical Society.

(E) DFT-predicted reaction energy diagram for hydrogenation of benzaldehyde in the absence of phenol.[21] Copyright 2020, John Wiley & Sons.

(F) DFT-predicted reaction energy diagram for hydrogenation of benzaldehyde in the presence of phenol on Pd(111). Calculations were performed on a charged surface with a charge density of approximately 0.01 e^- per surface Pd atom.[14] Copyright 2022, Elsevier.

experiments to obtain steady-state rate data are conducted for the organic mixture of R_1 and R_2 by varying their ratio at a constant pH and catalyst loading (normalized to the number of active sites). The EF is analyzed versus the concentration of R_2 at a constant R_1 concentration to check if there is an enhancement.

Kinetic modeling of experimental data may be able to identify simple mutual influences (Figure 3B). The proposed reaction mechanism for the organic mixture would be a combination of the two individual reaction mechanisms. If these enhancements are governed by simple mutual influences only, the rate constants for adsorption, desorption, and reactions for the hydrogenation/HDO of an organic mixture of R_1 and R_2 should be equal to the rate constants for their corresponding individual reactions. If the rate constants in the mixture of R_1 and R_2 compared to R_1 and R_2 individually are not equal, then we infer that complex mutual influences are involved (Figure 3C). For example, one study modeled separate LH mechanisms using steady-state HDO reaction data to describe the HDO of furfural and guaiacol

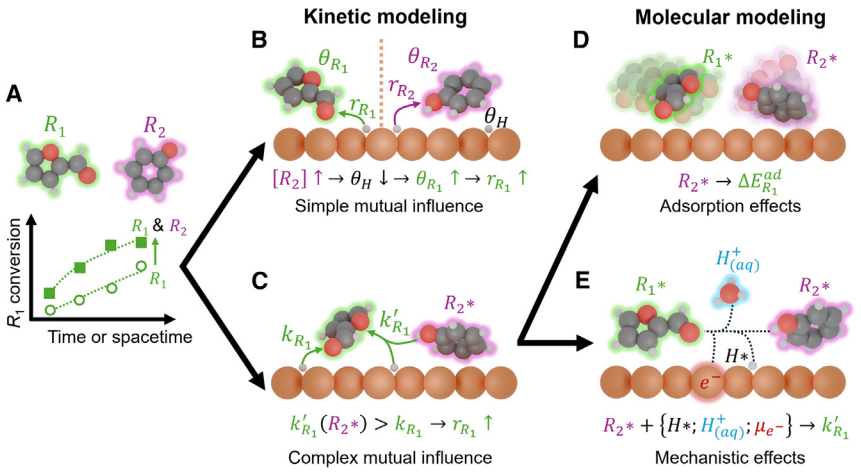

Figure 3. Understanding mutual influences of organics in (electro)catalysis

(A) Kinetic studies without transport artifacts are key to determine whether an enhancement is occurring. A control experiment under the same conditions is required to ensure any enhancements are not due to changes in the catalyst area or structure. Comparing the experimental kinetics to kinetic models can describe whether an enhancement can be explained by simple mutual influences.

(B) Simple mutual influences generally seem to occur when the coverage of R_1 is low in the absence of R_2 and require considerable conversion of R_2. The absence of conversion of R_2 with an EF > 1 may indicate complex mutual influences.

(C) Complex mutual influences are characterized by changes in the rate constants of elementary steps, denoted by k_{R_1} changing to k'_{R_1} in the presence of R_2*.

(D) Molecular modeling can predict adsorption energy changes for R_1 ($\Delta E^{ad}_{R_1}$) in the presence of a co-reactant R_2.

(E) Molecular modeling can also elucidate the effect of co-reactant R_2 on the energetics of R_1 reacting with surface protons ($H*$) or solution-phase protons ($H^+_{(aq)}$) and electrons (e^-).

individually and then used those data as a benchmark to identify synergistic effects in the HDO of a furfural-guaiacol mixture.[7] Since the rate constants for individual reactions and mixture reactions did not match, complex influences were deemed to be the reason for rate enhancement. Rather than modeling the entire set of rate constants, based on our analysis, a quick check of whether complex mutual influences are at play is to see if the enhancement in the rate is accompanied by an increase in reaction selectivity as well. This increase in reaction selectivity can be seen in cases where the conversion of R_2 is suppressed for R_1 enhancement, such as the suppression of phenol hydrogenation during the electrocatalytic hydrogenation of the benzaldehyde-phenol mixture.[15] However, simple and complex influences may affect reaction rates simultaneously, and, hence, a rigorous kinetics study is required to deconvolute these effects. For example, a weak synergistic complex mutual effect may be negated due to strong competitive adsorption between the reactants. Knowledge of the type of mutual influence impacting the reactants can be leveraged to optimize rate enhancements.

The kinetic model derived for the organic mixture can be used to determine the upper limit of the EF by simple mutual influences and the corresponding operating conditions. The EF for an LH reaction is maximized by varying the relative concentration of R_2 at a constant bulk pH. However, if the absolute rate of R_1 is small, then the bulk pH should first be tuned before tuning EF. Additionally, there is a tradeoff between EF and selectivity for simple mutual influences. Thus, careful thought should be put into choosing an optimal relative R_2 concentration and reaction conditions. For both thermocatalysis and electrocatalysis, given the same reaction mechanism and rate constants, the same EFs can be observed if only simple mutual influences are at play. However, the complex mutual influences will vary depending on the effects of temperature, applied electrochemical potential, solvent interactions, and overall reaction mechanisms.

Molecular modeling of single and multiple organic reactants can clarify mutual influences on adsorption energies and activation barriers. To accurately predict the adsorption thermodynamics and kinetics for these systems in (electro)catalytic reactions, it is important to consider solvent effects at the catalytic interface, which include solvation of reaction intermediates and participation of solvent molecules in the reaction mechanism. Solvent effects can be described either through a combination of implicit solvation and micro-solvation or fully explicit solvent.[26–29] Additionally, for electrocatalysis, the applied electrochemical potential plays a major role in modulating reaction energetics and, therefore, should be accounted for[30–33]; the applied potential can affect organics with dissimilar functional groups in different ways. To accurately model the effect of R_2 on the adsorption free energy of R_1 (Figure 3D), it is crucial to consider an ensemble of interactions between R_1 and R_2 using sampling techniques such as *ab initio* molecular dynamics. The species R_1 may be interacting with nearby R_2 in solution or with co-adsorbed R_2. The change in the R_1-R_2 interaction energy with different R_2 can elucidate trends on how the adsorption of R_1 will be modulated with R_2. When studying the complex mutual influence of R_2 on the reaction mechanism and kinetics of R_1, one should consider different possible mechanisms (Figure 3E) made possible by R_2 and compare them with the original mechanism in the absence of R_2.[14] Comparisons between modeling predictions and experimental observables such as equilibrium constants and apparent activation barriers, as well as predicted EFs, should be made whenever possible.

Concluding remarks

Simple and complex mutual influences can lead to increases in rates of (electro)catalytic conversion in organic mixtures. Based on literature reports, simple and complex mutual influences often have a similar magnitude of enhancement on the reaction rates of R_1 and R_2. Typical EF values observed for catalytic hydrogenation and HDO of R_1 in organic mixtures are a factor of 2–3 compared to R_1 alone, but this EF can possibly be made larger with proper tuning. Based on our microkinetic modeling, simple mutual influence can lead to an EF over 20 for certain regimes of rate constants and reactant concentrations but at the expense of product selectivity. A synergistic effect on R_1 via simple mutual influences can only occur if R_2 is reacting with adsorbed surface

species (e.g., H*); if a synergistic effect on the rate of reaction for R_1 is observed and R_2 is not reacting, then a complex mutual influence must be occurring. Complex mutual influences can enhance both activity and selectivity to the desired product, unlike simple mutual influences. Complex mutual influences can occur because of hydrogen bonding or van der Waals interactions between co-reactants, although a change in the local microenvironment near R_1 due to the inclusion of R_2 (e.g., change in local H_3O^+ concentration) also warrants further investigation. Without careful consideration, however, site blocking by R_2 could decrease the reaction rate of R_1 more than any enhancements through synergistic mutual influences. More knowledge about mutual influences will aid conversion of organic mixtures to renewable fuels and chemicals.

DATA AND CODE AVAILABILITY

A GitHub repository[13] with code has been prepared, and the URL is provided in the supplemental information statement.

ACKNOWLEDGMENTS

This material is based upon work supported by the National Science Foundation under grant 2320929. B.R.G. acknowledges the Office of Naval Research (N000142312439) for support. The authors thank Prof. Andrew Allman at the University of Michigan for his help with Pareto frontier optimization.

DECLARATION OF INTERESTS

The authors declare no competing interests.

SUPPLEMENTAL INFORMATION

Supplemental information can be found online at https://doi.org/10.1016/j.checat.2024.101135.

REFERENCES

1. Lee, K., Jing, Y., Wang, Y., and Yan, N. (2022). A unified view on catalytic conversion of biomass and waste plastics. Nat. Rev. Chem *6*, 635–652. https://doi.org/10.1038/s41570-022-00411-8.
2. Khemthong, P., Yimsukanan, C., Narkkun, T., Srifa, A., Witoon, T., Pongchaiphol, S., Kiatphuengporn, S., and Faungnawakij, K. (2021). Advances in catalytic production of value-added biochemicals and biofuels via furfural platform derived lignocellulosic biomass. Biomass Bioenergy *148*, 106033. https://doi.org/10.1016/j.biombioe.2021.106033.
3. Akhade, S.A., Singh, N., Gutiérrez, O.Y., Lopez-Ruiz, J., Wang, H., Holladay, J.D., Liu, Y., Karkamkar, A., Weber, R.S., Padmaperuma, A.B., et al. (2020). Electrocatalytic Hydrogenation of Biomass-Derived Organics: A Review. Chem. Rev. *120*, 11370–11419. https://doi.org/10.1021/acs.chemrev.0c00158.
4. Gollakota, A.R., Shu, C.-M., Sarangi, P.K., Shadangi, K.P., Rakshit, S., Kennedy, J.F., Gupta, V.K., and Sharma, M. (2023). Catalytic hydrodeoxygenation of bio-oil and model compounds - Choice of catalysts, and mechanisms. Renew. Sustain. Energy Rev. *187*, 113700. https://doi.org/10.1016/j.rser.2023.113700.
5. Pyatnitsky, Y.I. (1994). Some new approaches to the competitive catalytic reaction kinetics. Appl. Catal. Gen. *113*, 9–28. https://doi.org/10.1016/0926-860X(94)80238-6.
6. Sifontes Herrera, V.A., Saleem, F., Kusema, B., Eränen, K., and Salmi, T. (2012). Hydrogenation of l-Arabinose and d-Galactose Mixtures Over a Heterogeneous Ru/C Catalyst. Top. Catal. *55*, 550–555. https://doi.org/10.1007/s11244-012-9833-z.
7. Schiesser, E.C., Blanco, E., Dongil, A.B., Zarate, X., Saavedra-Torres, M., Schott, E., Canales, R.I., and Escalona, N. (2021). Insights into Hydrodeoxygenation of Furfural and Guaiacol Mixture: Experimental and Theoretical Studies. J. Phys. Chem. C *125*, 7647–7657. https://doi.org/10.1021/acs.jpcc.0c11415.
8. Liu, Z., Hamad, I.A., Li, Y., Chen, Y., Wang, S., Jentoft, R.E., and Jentoft, F.C. (2019). Poisoning and competitive adsorption effects during phenol hydrogenation on platinum in water-alcohol mixtures. Appl. Catal. Gen. *585*, 117199. https://doi.org/10.1016/j.apcata.2019.117199.
9. Ryymin, E.-M., Honkela, M.L., Viljava, T.-R., and Krause, A.I. (2010). Competitive reactions and mechanisms in the simultaneous HDO of phenol and methyl heptanoate over sulphided NiMo/γ-Al2O3. Appl. Catal. Gen. *389*, 114–121. https://doi.org/10.1016/j.apcata.2010.09.010.
10. Singh, N., Sanyal, U., Ruehl, G., Stoerzinger, K.A., Gutiérrez, O.Y., Camaioni, D.M., Fulton, J.L., Lercher, J.A., and Campbell, C.T. (2020). Aqueous phase catalytic and electrocatalytic hydrogenation of phenol and benzaldehyde over platinum group metals. J. Catal. *382*, 372–384. https://doi.org/10.1016/j.jcat.2019.12.034.
11. Akinola, J., Barth, I., Goldsmith, B.R., and Singh, N. (2024). Electrocatalytic hydrogenation of phenol on platinum-cobalt alloys. J. Catal. *430*, 115331. https://doi.org/10.1016/j.jcat.2024.115331.
12. The MathWorks Inc (2022). Optimization Toolbox Version: 9.4 (R2022b) (The MathWorks Inc.).
13. Halarnkar, S. (2024). https://github.com/sahilhalarnkar/Simple_Mutual_Influence.
14. Sanyal, U., Yuk, S.F., Koh, K., Lee, M.-S., Stoerzinger, K., Zhang, D., Meyer, L.C., Lopez-Ruiz, J.A., Karkamkar, A., Holladay, J.D., et al. (2021). Hydrogen Bonding Enhances the Electrochemical Hydrogenation of Benzaldehyde in the Aqueous Phase. Angew. Chem. Int. Ed. Engl. *60*, 290–296. https://doi.org/10.1002/anie.202008178.
15. Liang, L., Wang, C., Lu, X., Sun, Y., Yan, B., Li, N., Chen, G., and Hou, L. (2024). Interactions of phenol and benzaldehyde in electrocatalytic upgrading process. Chin. Chem. Lett. *35*, 108581. https://doi.org/10.1016/j.cclet.2023.108581.
16. Anibal, J., and Xu, B. (2020). Electroreductive C–C Coupling of Furfural and Benzaldehyde on Cu and Pb Surfaces. ACS Catal. *10*, 11643–11653. https://doi.org/10.1021/acscatal.0c03110.
17. Guo, M., Jayakumar, S., Luo, M., Kong, X., Li, C., Li, H., Chen, J., and Yang, Q. (2022). The promotion effect of π-π interactions in Pd NPs catalysed selective hydrogenation. Nat. Commun. *13*, 1770. https://doi.org/10.1038/s41467-022-29299-0.
18. Taft, R.W., Gurka, D., Joris, L., Schleyer, P.v.R., and Rakshys, J.W. (1969). Studies of hydrogen-bonded complex formation with p-fluorophenol. V. Linear free energy relationships with OH reference acids. J. Am. Chem. Soc. *91*, 4801–4808. https://doi.org/10.1021/ja01045a038.
19. Madushanka, A., Moura, R.T., Verma, N., and Kraka, E. (2023). Quantum Mechanical Assessment of Protein–Ligand Hydrogen Bond Strength Patterns: Insights from Semiempirical Tight-Binding and Local Vibrational Mode Theory. Int. J. Mol. Sci. *24*, 6311. https://doi.org/10.3390/ijms24076311.
20. Sanyal, U., Koh, K., Meyer, L.C., Karkamkar, A., and Gutiérrez, O.Y. (2021). Simultaneous electrocatalytic hydrogenation of aldehydes and phenol over carbon-supported metals. J. Appl. Electrochem. *51*, 27–36. https://doi.org/10.1007/s10800-020-01464-7.
21. Yuk, S.F., Lee, M.-S., Akhade, S.A., Nguyen, M.-T., Glezakou, V.-A., and Rousseau, R. (2022). First-principle investigation on catalytic hydrogenation of benzaldehyde over Pt-group metals. Catal. Today *388–389*, 208–215. https://doi.org/10.1016/j.cattod.2020.07.039.
22. Akinola, J., Barth, I., Goldsmith, B.R., and Singh, N. (2020). Adsorption Energies of Oxygenated Aromatics and Organics on Rhodium and Platinum in Aqueous Phase. ACS Catal. *10*, 4929–4941. https://doi.org/10.1021/acscatal.0c00803.

23. Garedew, M., Young-Farhat, D., Jackson, J.E., and Saffron, C.M. (2019). Electrocatalytic Upgrading of Phenolic Compounds Observed after Lignin Pyrolysis. ACS Sustainable Chem. Eng. *7*, 8375–8386. https://doi.org/10.1021/acssuschemeng.9b00019.

24. Tian, C., Dorakhan, R., Wicks, J., Chen, Z., Choi, K.-S., Singh, N., Schaidle, J.A., Holewinski, A., Vojvodic, A., Vlachos, D.G., et al. (2024). Progress and roadmap for electro-privileged transformations of bio-derived molecules. Nat. Catal. *7*, 350–360. https://doi.org/10.1038/s41929-024-01131-6.

25. Meylemans, H.A., Quintana, R.L., and Harvey, B.G. (2012). Efficient conversion of pure and mixed terpene feedstocks to high density fuels. Fuel *97*, 560–568. https://doi.org/10.1016/j.fuel.2012.01.062.

26. Ringe, S., Hörmann, N.G., Oberhofer, H., and Reuter, K. (2022). Implicit Solvation Methods for Catalysis at Electrified Interfaces. Chem. Rev. *122*, 10777–10820. https://doi.org/10.1021/acs.chemrev.1c00675.

27. Yang, G., Maliekkal, V., Chen, X., Eckstein, S., Shi, H., Camaioni, D.M., Baráth, E., Haller, G.L., Liu, Y., Neurock, M., and Lercher, J.A. (2021). Rate enhancement of phenol hydrogenation on Pt by hydronium ions in the aqueous phase. J. Catal. *404*, 579–593. https://doi.org/10.1016/j.jcat.2021.11.003.

28. Zhao, Z., Bababrik, R., Xue, W., Li, Y., Briggs, N.M., Nguyen, D.-T., Nguyen, U., Crossley, S.P., Wang, S., Wang, B., and Resasco, D.E. (2019). Solvent-mediated charge separation drives alternative hydrogenation path of furanics in liquid water. Nat. Catal. *2*, 431–436. https://doi.org/10.1038/s41929-019-0257-z.

29. Yao, Z., Xia, G.-J., Cao, W., Zeng, K.-H., and Wang, Y.-G. (2023). Mechanistic exploration of furfural hydrogenation on copper surface in aqueous phase by DFT and AIMD simulations. J. Catal. *418*, 1–12. https://doi.org/10.1016/j.jcat.2022.12.024.

30. Agrawal, N., Wong, A.J.-W., Maheshwari, S., and Janik, M.J. (2024). An efficient approach to compartmentalize double layer effects on kinetics of interfacial proton-electron transfer reactions. J. Catal. *430*, 115360. https://doi.org/10.1016/j.jcat.2024.115360.

31. Sundararaman, R., Vigil-Fowler, D., and Schwarz, K. (2022). Improving the Accuracy of Atomistic Simulations of the Electrochemical Interface. Chem. Rev. *122*, 10651–10674. https://doi.org/10.1021/acs.chemrev.1c00800.

32. Wu, Q., Dai, C., Meng, F., Jiao, Y., and Xu, Z.J. (2024). Potential and electric double-layer effect in electrocatalytic urea synthesis. Nat. Commun. *15*, 1095. https://doi.org/10.1038/s41467-024-45522-6.

33. Tezak, C.R., Singstock, N.R., Alherz, A.W., Vigil-Fowler, D., Sutton, C.A., Sundararaman, R., and Musgrave, C.B. (2023). Revised Nitrogen Reduction Scaling Relations from Potential-Dependent Modeling of Chemical and Electrochemical Steps. ACS Catal. *13*, 12894–12903. https://doi.org/10.1021/acscatal.3c01978.

Chem Catalysis, Volume *4*

Supplemental information

Synergistic effects in organic mixtures for enhanced catalytic hydrogenation and hydrodeoxygenation

Ankit Mathanker, Sahil Halarnkar, Bolton Tran, Nirala Singh, and Bryan R. Goldsmith

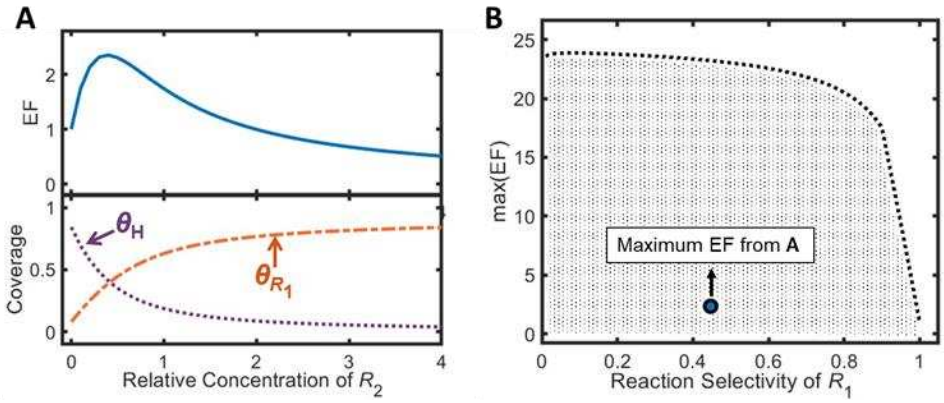

Figure S1. Enhancement factor through simple mutual influence for Eley-Rideal
(A) The enhancement factor (EF, blue) versus relative R_2 concentration (= C_{R_2}/C_{R_1}), alongside coverages for R_1 (dot-dashed orange line) and H (dotted purple line). Values of rate constants and concentrations are: C_{R_1} = 1, C_H= 1, k_{S15} = 2, k_{-S15} = 0.1, k_{S16} = 1, k_{-S16} = 0.1, k_{S17} = 1, k_{S18} = 1.2.
(B) Pareto front to maximize EF for different values of R_1 selectivity (= $r_{R_1}/[r_{R_1} + r_{R_2}]$). The dotted line represents the maximum EF that can be obtained from simple mutual influences under the bounds used here. The bounds used for the rate parameters and concentrations are [0.01, 10] and [0.01, 1], respectively. The highest EF value from Figure S1(A) is denoted by a blue circle marker.

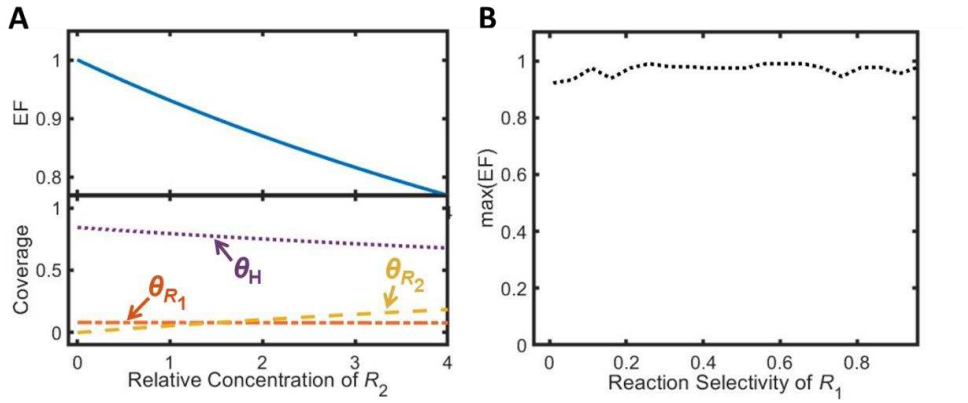

Figure S2. Enhancement factor through simple mutual influence for proton-coupled electron transfer (PCET)
(A) The enhancement factor (EF, blue) versus relative R_2 concentration (= C_{R_2}/C_{R_1}), alongside coverages for R_1 (dot-dashed orange line) and H (dotted purple line). Values of rate constants and concentrations are: C_{R_1} = 1, C_H= 1, k_{S22} = 2, k_{-S22} = 0.1, k_{S23} = 1, k_{-S23} = 0.1, k_{S24} = 1, k_{S25} = 1, k_{-S25} = 0.1, k_{S26} = 1.2.
(B) Pareto front to maximize EF for different values of R_1 selectivity (= $r_{R_1}/[r_{R_1} + r_{R_2}]$). The dotted line represents the maximum EF that can be obtained from simple mutual influences under the bounds used here. The bounds used for the rate parameters and concentrations are [0.01, 10] and [0.01, 1], respectively.

Table S1. All enhancement factors reviewed in perspective.

R_1	R_2	Reaction conditions and reaction	Catalyst	Maximum EF
NO [1]	O_2	Reduction by CO in gas phase	Pd	2 for N_2; 1.5 for N_2O
Benzaldehyde [2]	Phenol	Sodium acetate (3M, pH 5.2), 20 mM R_1 and 20 mM R_2, 298 K, 1 bar N_2, −0.1 V vs. RHE	Pd/C	3.2
	2-Fluorophenol			2.6
	Benzoic acid			1.8

Furfural [3]	Guaiacol	R_1 = 0.23 mol L^{-1}, 250 °C, 5 MPa of H_2, 300 mL batch reactor with 80 mL dioxane and 700 µL hexadecane	Ni/SiO_2	2.7 (R_2 = 5.8 mol L^{-1}) 2.5 (R_2 = 4.6 mol L^{-1}) 2.2 (R_2 = 3.5 mol L^{-1}) 1.9 (R_2 = 2.3 mol L^{-1}) 1.7 (R_2 = 1.8 mol L^{-1})

Note S1. Langmuir-Hinshelwood rate law derivation assuming that all adsorption steps are quasi-equilibrated

A set of five elementary steps describing Langmuir-Hinshelwood (LH) reactions involving two co-reactants may be:

$$\mathrm{H} + * \rightleftarrows \mathrm{H}* \tag{1}$$

$$R_1 + * \rightleftarrows R_1* \tag{2}$$

$$\mathrm{H}* + R_1* \longrightarrow 2* + R_1\mathrm{H} \tag{3}$$

$$R_2 + * \rightleftarrows R_2* \tag{4}$$

$$\mathrm{H}* + R_2* \longrightarrow 2* + R_2\mathrm{H} \tag{5}$$

where H represents a hydrogen equivalent that competes for free sites (*) with reactant R_1 and co-reactant R_2. Here we assume that all adsorption steps are quasi-equilibrated. This gives the following equilibrium constant K_i relations, where i denotes the i^{th} adsorption step:

$$K_1 = \frac{\theta_{\mathrm{H}}}{C_{\mathrm{H}}\theta_*} \tag{S1}$$

$$K_2 = \frac{\theta_{R_1}}{C_{R_1}\theta_*} \tag{S2}$$

$$K_4 = \frac{\theta_{R_2}}{C_{R_2}\theta_*} \tag{S3}$$

The site balance equation is: $1 = \theta_* + \theta_{\mathrm{H}} + \theta_{R_1} + \theta_{R_2}$, where θ_X is the coverage of species X and sums to 1 such that the rate is normalized to the total number of catalytic sites on the surface. The site balance is rewritten in terms of equilibrium constants and bulk species concentrations:

$$1 = \theta_* + K_1 C_{\mathrm{H}}\theta_* + K_2 C_{R_1}\theta_* + K_4 C_{R_2}\theta_* \tag{S4}$$

$$\theta_* = \frac{1}{1 + K_1 C_{\mathrm{H}} + K_2 C_{R_1} + K_4 C_{R_2}} \tag{S5}$$

The rate law for the elementary hydrogenation step (3) for R_1 is:

$$r_{R_1} = k_3 \theta_{R_1} \theta_{\mathrm{H}} = k_3 K_2 C_{R_1} K_1 C_{\mathrm{H}} \theta_*^2 \tag{S6}$$

Substituting the expression for θ_* gives the final rate law expression if step 3 is rate-determining:

$$r_{R_1} = \frac{k_3 K_2 K_1 C_{R_1} C_{\mathrm{H}}}{(1 + K_1 C_{\mathrm{H}} + K_2 C_{R_1} + K_4 C_{R_2})^2} \tag{6}$$

Note S2. Langmuir-Hinshelwood rate law derivation assuming pseudo-steady-state hypothesis to catalytic intermediates to capture simple mutual influences

The simple mutual influence is only explained by a rate law if we do not assume that adsorption steps are quasi-equilibrated. By applying the pseudo-steady-steady hypothesis (PSSH) to the adsorbed species, the derived rate for R_1 can be increased by the presence of R_2.

The rate of each elementary step is written as:

$$r_1 = k_1 C_{\mathrm{H}} \theta_* - k_{-1} \theta_{\mathrm{H}} \quad \text{(S7)}$$

$$r_2 = k_2 C_{R_1} \theta_* - k_{-2} \theta_{R_1} \quad \text{(S8)}$$

$$r_3 = r_{R_1} = k_3 \theta_{R_1} \theta_{\mathrm{H}} \quad \text{(S9)}$$

$$r_4 = k_4 C_{R_2} \theta_* - k_{-4} \theta_{R_2} \quad \text{(S10)}$$

$$r_5 = r_{R_2} = k_5 \theta_{R_2} \theta_{\mathrm{H}} \quad \text{(S11)}$$

The rate constants k_i and k_{-i} are the forward and reverse rates constants for elementary step i (reversible steps in Eq. 1, 2, 4 and irreversible steps Eq. 3, 6). The rate of reaction r_i in Eq. S7-S11 corresponds to the elementary steps in Eq. 1-6.

The PSSH requires the concentration of surface intermediates R_1^*, R_2^* and H^* to be constant with time. This condition allows us to set the time derivatives of θ_{R_1}, $\theta_{R_2}$and θ_{H} to zero and obtain a system of algebraic equations:

$$\frac{d\theta_{R_1}}{dt} = r_2 - r_3 = k_2 C_{R_1} \theta_* - k_{-2} \theta_{R_1} - k_3 \theta_{R_1} \theta_{\mathrm{H}} \approx 0 \quad \text{(S12)}$$

$$\frac{d\theta_{R_2}}{dt} = r_4 - r_5 = k_4 C_{R_2} \theta_* - k_{-4} \theta_{R_2} - k_5 \theta_{R_2} \theta_{\mathrm{H}} \approx 0 \quad \text{(S13)}$$

$$\frac{d\theta_{\mathrm{H}}}{dt} = r_1 - r_3 - r_5 = k_1 C_{\mathrm{H}} \theta_* - k_{-1} \theta_{\mathrm{H}} - k_3 \theta_{R_1} \theta_{\mathrm{H}} - k_5 \theta_{R_2} \theta_{\mathrm{H}} \approx 0 \quad \text{(S14)}$$

Along with the site balance equation $1 = \theta_* + \theta_{\mathrm{H}} + \theta_{R_1} + \theta_{R_2}$, there are four algebraic equations to solve with four variables $(\theta_*, \theta_{\mathrm{H}}, \theta_{R_1} \& \theta_{R_2})$. The MATLAB solver lsqnonlin is used to solve for the system of equations, following which equations S9 and S11 are used to find the rate of hydrogenation of R_1 and R_2, respectively. The results are presented in **Figure 1**.

Note S3. Eley-Rideal rate law derivation assuming pseudo-steady-state hypothesis to capture simple mutual influences

It is possible for reactant R_1 to display simple mutual enhancements when reactant R_2 follows an Eley-Rideal mechanism.

$$\mathrm{H} + * \rightleftarrows \mathrm{H}* \quad \text{(S15)}$$

$$R_1 + * \rightleftarrows R_1* \quad \text{(S16)}$$

$$\mathrm{H}* + R_1* \longrightarrow 2* + R_1\mathrm{H} \quad \text{(S17)}$$

$$\mathrm{H}* + R_2 \longrightarrow * + R_2\mathrm{H} \quad \text{(S18)}$$

Assuming the PSSH holds for surface intermediates R_1^* and H^*, the system of algebraic equations reduces to:

$$\frac{d\theta_{R_1}}{dt} = r_{\mathrm{S16}} - r_{\mathrm{S17}} = k_{\mathrm{S16}} C_{R_1} \theta_* - k_{-\mathrm{S16}} \theta_{R_1} - k_{\mathrm{S17}} \theta_{R_1} \theta_{\mathrm{H}} \approx 0 \quad \text{(S19)}$$

$$\frac{d\theta_{\mathrm{H}}}{dt} = r_{\mathrm{S15}} - r_{\mathrm{S17}} - r_{\mathrm{S18}} = k_{\mathrm{S15}} C_{\mathrm{H}} \theta_* - k_{-\mathrm{S15}} \theta_{\mathrm{H}} - k_{\mathrm{S17}} \theta_{R_1} \theta_{\mathrm{H}} - k_{\mathrm{S18}} C_{R_2} \theta_{\mathrm{H}} \approx 0 \quad \text{(S20)}$$

$$1 = \theta_* + \theta_{\mathrm{H}} + \theta_{R_1} \quad \text{(S21)}$$

Similar to **Note S2.,** MATLAB function lsqnonlin was used to solve for steady state coverages. The results are presented in **Figure S1**.[4]

Note S4. PCET rate law derivation assuming pseudo-steady-state hypothesis to capture simple mutual influences

The PCET mechanism, where bulk H reacts with surface intermediate R_2^*, does not display simple mutual effects for reactant R_1.

$$\mathrm{H} + * \rightleftarrows \mathrm{H}* \quad \text{(S22)}$$

$$R_1 + * \rightleftarrows R_1* \quad \text{(S23)}$$

$$\mathrm{H}* + R_1* \longrightarrow 2* + R_1\mathrm{H} \quad \text{(S24)}$$

$$R_2 + * \rightleftarrows R_2* \quad \text{(S25)}$$

$$\mathrm{H} + R_2* \longrightarrow * + R_2\mathrm{H} \quad \text{(S26)}$$

Assuming the PSSH holds for surface intermediates R_1^*, R_2^* and H*, the system of algebraic equations reduces to:

$$\frac{d\theta_{R_1}}{dt} = r_{\mathrm{S23}} - r_{\mathrm{S24}} = k_{\mathrm{S23}} C_{R_1} \theta_* - k_{-\mathrm{S23}} \theta_{R_1} - k_{\mathrm{S24}} \theta_{R_1} \theta_{\mathrm{H}} \approx 0 \quad \text{(S27)}$$

$$\frac{d\theta_{R_2}}{dt} = r_{\mathrm{S25}} - r_{\mathrm{S26}} = k_{\mathrm{S25}} C_{R_2} \theta_* - k_{-\mathrm{S25}} \theta_{R_2} - k_{S26} \theta_{R_2} C_{\mathrm{H}} \approx 0 \quad \text{(S28)}$$

$$\frac{d\theta_{\mathrm{H}}}{dt} = r_{\mathrm{S22}} - r_{\mathrm{S24}} - r_{\mathrm{S26}} = k_{\mathrm{S22}} C_{\mathrm{H}} \theta_* - k_{-\mathrm{S22}} \theta_{\mathrm{H}} - k_{\mathrm{S24}} \theta_{R_1} \theta_{\mathrm{H}} - k_{\mathrm{S26}} \theta_{R_2} C_{\mathrm{H}} \approx 0 \quad \text{(S29)}$$

$$1 = \theta_* + \theta_{\mathrm{H}} + \theta_{R_1} + \theta_{R_2} \quad \text{(S30)}$$

Similar to **Note S2.,** MATLAB function lsqnonlin was used to solve for steady state coverages. The results are presented in **Figure S2**. We see that the maximum EF that can be obtained through optimization does not cross 1, indicating no synergistic simple mutual influence.

Note S5. Generating the Pareto front

In multi-objective optimization, a Pareto front is the set of solutions that optimize for one objective function while limiting the marginal loss in other objective functions. The formulation of this problem is as follows:

$$max(f_1(x), f_2(x), f_3(x), \ldots f_n(x))$$

$$s.t\ x \in S$$

where x is the vector of decision variables, $f_1(x)$, … , $f_n(x)$ are the n objective functions and S is the feasible region.[5]

We use the ϵ - constraint method to obtain the Pareto front. The formal definition of the method is as follows:

$$max(f_1(x))$$

$$s.t$$

$$f_2(x) \geq \epsilon$$

$$f_3(x) \geq \epsilon$$

$$\ldots$$

$$f_n(x) \geq \epsilon$$

$$x \in S$$

In this case, $f_1(x)$ is the EF (enhancement factor), $f_2(x)$ is the reaction selectivity of R_1 and S is the set of all possible values for the rate constants and concentrations in the model.

The ϵ - constraint method is implemented using the optimproblem scheme present in the Optimization Toolbox in MATLAB.[6] The Pareto front depends strongly on the bounds set for the rate constants and concentrations.

References

1. Pyatnitsky, Yu.I. (1994). Some new approaches to the competitive catalytic reaction kinetics. Appl. Catal. Gen. *113*, 9–28. https://doi.org/10.1016/0926-860X(94)80238-6.

2. Sanyal, U., Yuk, S.F., Koh, K., Lee, M.-S., Stoerzinger, K., Zhang, D., Meyer, L.C., Lopez-Ruiz, J.A., Karkamkar, A., Holladay, J.D., et al. (2021). Hydrogen Bonding Enhances the Electrochemical Hydrogenation of Benzaldehyde in the Aqueous Phase. Angew. Chem. Int. Ed. *60*, 290–296. https://doi.org/10.1002/anie.202008178.

3. Schiesser, E.C., Blanco, E., Dongil, A.B., Zarate, X., Saavedra-Torres, M., Schott, E., Canales, R.I., and Escalona, N. (2021). Insights into Hydrodeoxygenation of Furfural and Guaiacol Mixture: Experimental and Theoretical Studies. J. Phys. Chem. C *125*, 7647–7657. https://doi.org/10.1021/acs.jpcc.0c11415.

4. Halarnkar, S. (2024). https://github.com/sahilhalarnkar/Simple_Mutual_Influence.

5. Mavrotas, G. (2009). Effective implementation of the *ε*-constraint method in Multi-Objective Mathematical Programming problems. Appl. Math. Comput. *213*, 455–465. https://doi.org/10.1016/j.amc.2009.03.037.

6. The MathWorks Inc. (2022). Optimization Toolbox version: 9.4 (R2022b). (The MathWorks Inc.).